Engineering Geology 259 (2019) 105191

Contents lists available at ScienceDirect

Engineering Geology

journal homepage: www.elsevier.com/locate/enggeo

Stability analysis of landslide dams under surge action based on large-scale flume experiments

Ming Peng[a,b], Qiu-Lu Jiang[a,b], Qing-Zhao Zhang[a,b,*], Yi Hong[c], Ming-zi Jiang[a,b], Zhen-Ming Shi[a,b], Li-Min Zhang[d]

[a] Key Laboratory of Geotechnical and Underground Engineering of the Ministry of Education, Department of Geotechnical Engineering, Tongji University, Shanghai 200092, China
[b] Department of Geotechnical Engineering, College of Civil Engineering, Tongji University, Shanghai 200092, China
[c] Key Laboratory of Offshore Geotechnics and Material of Zhejiang Province, College of Civil Engineering and Architecture, Zhejiang University, Hangzhou, Zhejiang 310058, China
[d] Department of Civil and Environmental Engineering, the Hong Kong University of Science and Technology, HKSAR, Hong Kong, China

ARTICLE INFO

Keywords:
Landslide dam
Landslide lake
Surge waves
Dam breaching test
Dam failure

ABSTRACT

In recent years, large magnitude earthquakes have caused the formation of a large number of landslide dams. The rising water level in the landslide lakes may induce a large number of landslides in the lake areas. When landslides rush into a lake area, large-scale surges may be produced and would then strongly impact on the dam stability and cause a breaching process. To understand the erosion failure modes of dam bodies caused by surges and the variation in the pore water pressure in the dam body, large-scale wave flume tests were carried out in this study. Six groups of comparative tests were carried out to study the two main influencing factors, namely, the upstream water level and the wave height. It was found that (1) when subjected to surge waves, the landslide dam stability is determined by the difference (ΔH) between the effective water level (the sum of the water level and the overlapping wave height) and the effective dam height (the dam height after lowering due to local sliding); (2) when $\Delta H < 0$, overtopping does not occur, and the landslide dam remains stable. A stable upstream erosion surface eventually forms, the surface slope angle decreases and the erosion volume increases as the wave height increases; when $\Delta H > 0$, the dam is overtopped and breached by the next waves; (3) During dam breach by overtopping with surge waves, the erosion in the breach initiation phase is much faster than by overtopping without surge waves, but the difference in the breaching development phase is not very significant; and (4) the pore water pressure close to the upstream slope is much more sensitive to the action of the surge waves than deeper inside the dam body.

1. Introduction

A landslide dam is formed by blockage of rivers with the soil and rock materials from landslides, avalanches, debris flows etc., which are triggered by earthquakes, rainfalls, snowmelts etc. (Peng and Zhang, 2012). In recent years, high magnitude earthquakes have caused the formation of a large numbers of landslide dams. The naturally-formed lake is called landslide lake or barrier lake. After the formation of a barrier lake, a rapid rise in the water level may cause a large number of landslides. When a landslide slides into the lake, it may produce huge surge waves (Hager et al., 2004; Koo and Kim, 2008). The surge may greatly erode the landslide dam, causing a much more rapid dam break and more serious flooding than that under normal conditions, which could be a great threat to human life and property downstream (Blown and Church, 1985; Evans and Clague, 1994; Soares-Frazão and Zech, 2007).

A landslide of 300 million m^3 slid into the Vaiont Reservoir in Italy in 1963, causing a tragic surge with wave heights as high as 300 m. The surge wave spread 1.4 km in 7 min and killed 3000 people in five towns (Tang and Lee, 1992). In 1983, a glacial avalanche rushed into the Homathko River in British Columbia, Canada. The surge caused by the avalanche overtopped a moraine dam and released a volume of water as large as 6 million m^3. Actually, the largest existing landslide dam, lake Sarez formed in Tajikistan in 1911 with a height of 800 m and a lake volume of 17 billion m^3, is threatened by an enormous potential landslide in the lake area only several kilometers upstream of the dam. In

* Corresponding author at: Key Laboratory of Geotechnical and Underground Engineering of the Ministry of Education, Department of Geotechnical Engineering, Tongji University, Shanghai 200092, China
E-mail address: zhangqingzhao@tongji.edu.cn (Q.-Z. Zhang).

https://doi.org/10.1016/j.enggeo.2019.105191
Received 30 September 2018; Received in revised form 1 June 2019
Available online 11 June 2019
0013-7952/

(a) Wave flow flume test platform

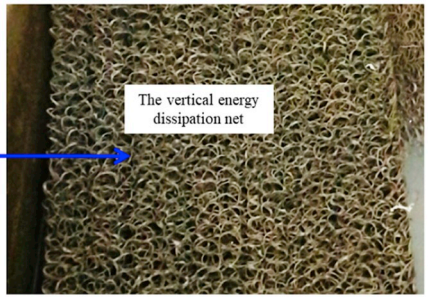

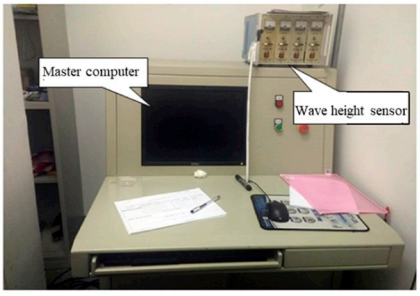

(b) Wave generating machine (c) Control computer

Fig. 1. Experimental system.

recent years, under the influence of earthquake activity and extreme climate disasters, landslide dams have occurred at an increasing rate worldwide (Cui et al., 2009; Waragai and Kajiyama, 2011; Huang et al., 2013; Liu et al., 2013). Thus, it is of great significance to study landslide dam stability under surge action.

The stability of landslide dams subjected to overtopping and overflow under natural conditions has been studied extensively (Yang et al., 2011; Niu et al., 2012; Peng and Zhang, 2012; Zhou et al., 2013, 2015), and much knowledge has been accumulated about the static stability. However, the study of surges caused by landslides and other external forces is still in its infancy (Shi et al., 2014, 2015). Some scholars use the theoretical calculation method to study the surge volume and the flood peak flow produced by the surge wave over the dam crest. For example, Risley et al. (2006) studied the amount of wave overtopping and the peak discharge of floods caused by the overtopping of a dam. Sattar et al. (2012) conducted a run-off analysis of the outflow hydrograph to evaluate the effect of the inundation levels of the flood wave on the failure of a dam. A numerical analysis, such as possible with the ISPH model, can be used to study the process of landslide surge generation, spread and overtopping of the dam (Lin et al., 2015). Demirel and Aydin (2016) and Xiao and Lin (2016) used the VOF numerical method to simulate the spreading process of a landslide surge and obtained the corresponding maximum wave height.

Model tests are also used to study the wave load of the landslide surge wave on the dam and the scour characteristics of the dam. Wiegel (1970) carried out an experimental study on landslide wave surges and studied the effects of the water depth, submerged volume, weight of the slide and inclination angle of the slope on the characteristics of the surge waves. Xu et al. (2015) studied and described the erosion failure characteristics of a dam in different scenarios of varying landslide surface area, landslide thickness and distances from the landslide entry point to the dam site. Chen et al. (2015) studied the wave loads on the downstream face of dams caused by different landslide entry angles and distances from the landslide entry point to the dam site as well as the geometry of the landslide body.

Although much efforts have been devoted to the effects of erosion characteristics of landslide wave surges on dams, the related studies only produced qualitative descriptions of the effects of the erosion characteristics of waves on the dam. Few researchers have measured the variation of pore water pressure in structures during a surge impact (Yamamoto et al., 1978; Madsen, 1978; Weoncheol and Kim 2008). Consequently, the mechanisms of dam surface erosion under surge waves, and the influence of the wave on the failure mode and dam stability has not been analyzed.

Therefore, in our investigations we studied, the landslide dam stability under a landslide wave surge in depth through large-scale wave

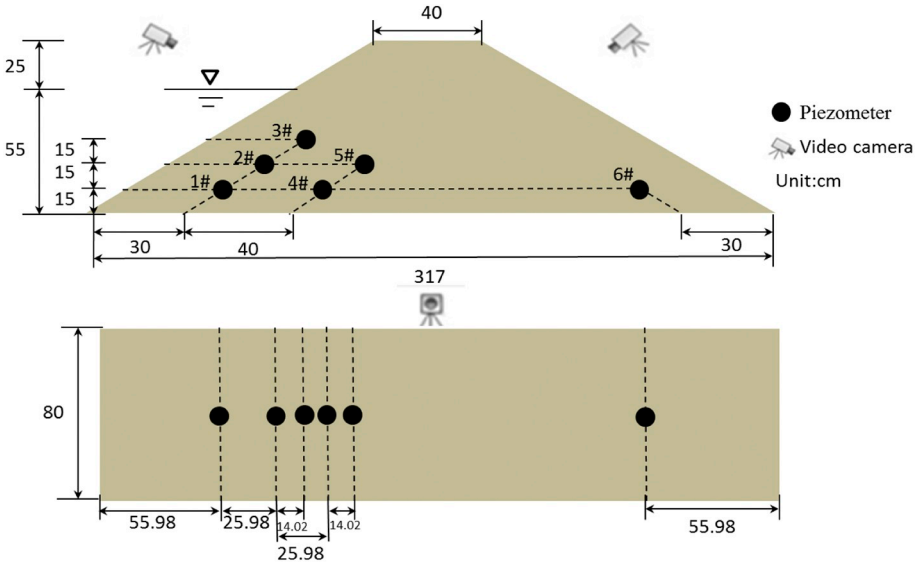

Fig. 2. The model dam and the test layout with a water level of 55 cm.

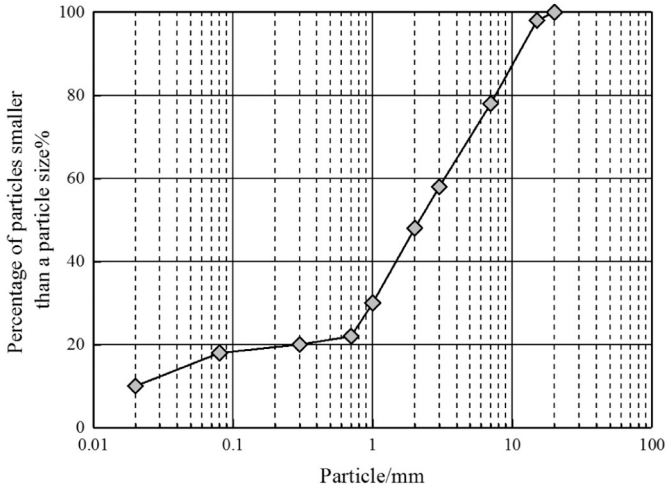

Fig. 3. Grain size distribution curve of the Donghekou landslide dam material.

flume testing with different water levels and wave heights. The characteristics of wave erosion and pore water pressure, on the basis of the experimental data, were studied to reveal the surge impact on the stability of the dam. Our paper provide a theoretical basis for approaches to control geological disasters involving a landslide dam and for the effective protection of human life and property in the downstream area.

The experiments were not designed to be a scale model of a specific landslide dam. According to the research of Xu et al. (2009), Peng et al. (2014), the scale and shape of the dams formed during the Wenchuan earthquake is widely varying. The height of the dams ranges from several meters to > 100 m (such as the Laoyangyan landslide dam), and the volume of the dams ranges from tens of thousands of cubic meters to 20.4 million cubic meters (for Tangjiashan landslide dam). The purpose of our study was to discuss the influence of the variation of the lake water level and wave height on the stability of dams in general terms, and not to study the behaviour of specific dams, so we did not use a well-defined scale factor in our experiments.

Table 1
Six test scenarios to study the impact of wave surges on a dam surge impact on a dam.

Scenario	Water level (cm)	Wave height (cm)	Dam material	Wave form
1	55	5	Donghekou landslide dam	Sine wave
2		10		
3		20		
4	75	5		
5		10		
6		20		

2. Wave flume experiment

2.1. Experimental flume and instrument

All tests are carried out in the wave flume system located at Tongji University. As shown in Fig. 1a, the length, width and depth of the flume are 42 m, 0.8 m and 1.25 m, respectively. The gradient of the flume bottom is zero. The bottom, head and tail of the flume are concrete structures, and the middle section is a steel structure. Through the transparent glass on both sides of the flume, the experimental phenomena in the flume can be observed directly during the experiments.

The wave generating system is located at the head of the wave flume, as shown in Fig. 1a. A vertical energy dissipation net is arranged at the back side of the wave-generating machine (Fig. 1b), and an energy dissipation slope is arranged at the other end of the flume to eliminate wave reflections. The wave generator can simulate regular waves, elliptical cosine waves, solitary waves, superimposed breaking waves, etc. The range for wave heights is 0.02–0.3 m. The wave height tester is monitored by a wave height sensor and a wave height amplifier, which are mainly used to monitor the water surface (Grilli and Watts, 1999).

The control computer is a PIV dual-core 2.6 GHz compatible machine (Fig. 1c), which is mainly used for calculation, analysis, wave-making control and data acquisition. It is connected to the control computer using a special control network line, through which the wave-making data files, the operational status of the servo system and other information are transmitted.

During the model test, the pore water pressure is measured by KPE-200KPB miniature piezometers with a measurement range of 200 kPa, which have good anti-interference characteristics and are capable of

Table 2
Model test results of the 6 scenarios, showing effective water level, effective dam height, and dam stability under wave surge impact.

Scenario	Water depth (cm)	Wave height (cm)	Effective water level (H_{we}) before dam (cm)[a]	Effective dam height (H_{de}) (cm)[b]	$\Delta H = H_{we} - H_{de}$ (cm)	Stability
1	55	5	60	80	-20	Stable
2		10	65	80	−15	Stable
3		20	75	73	2	Failed
4	75	5	80	78	2	Failed
5		10	85	75	10	Failed
6		20	95	74	21	Failed

[a] The effective water level is the sum of the water level and the overlapping wave height, which is approximated as the sum of the water level and the wave height. In the tests, the overlapping wave height is in reality 0–2 cm higher than the wave height shown in column 3.
[b] The effective dam height is defined as the height of the highest point of the dam body before it breaks down to the extent that a significant overflow occurs.

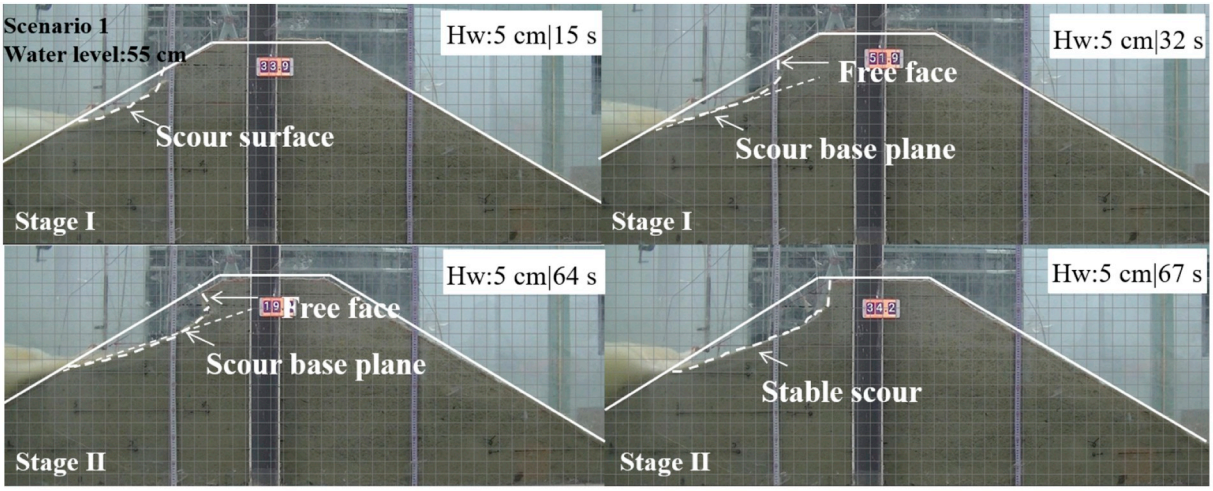

(a) Photographs of the different stages of Scenario 1

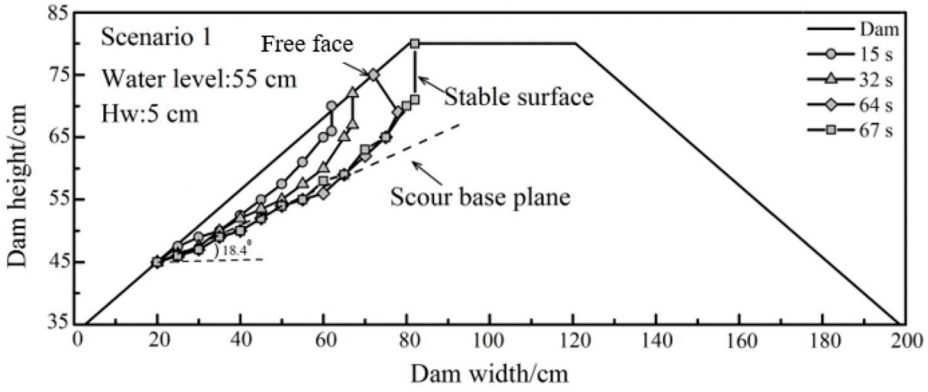

(b) Development of dam erosion in Scenario 1

Fig. 4. Scenario 1.

producing accurate measurements. The dynamic data are acquired by a small multi-channel data acquisition instrument, made by the Japan TML company, which has a sampling speed of up to 100 kHz. It is capable of withstanding vibrations and can be connected to the PC through a USB interface. The cameras used in the experiment are JVC GZ-R10BAC, which can record the whole experiment in the 1920*1080 high-definition mode of AVCHD. They are used to record the behavior of the dam and water level under the surge impact.

2.2. Dam model and material

The size and shape of the dam are varied. However, to study the general mechanics which affect the stability of the dam, this study did not select a specific dam as a prototype. Due to the size limitations of the flume, the dam body is modeled as a trapezoid, the bottom length is (along the stream direction) 317 cm, the crest length is 40 cm, the height is 80 cm, the river width is 80 cm, and the upstream and downstream slope of the dam faces is 30° (Xu et al., 2009; Peng et al., 2014). Six piezometers are arranged in the dam model to collect the pore water pressure data. Three high-definition cameras are arranged upstream, downstream and in front of the dam to monitor the displacements (Fig. 2).

The typical gradation curve of the Donghekou landslide dam in China is selected to prepare the dam material, as shown in Fig. 3 (Chang and Zhang, 2010; Xiong et al., 2018). The materials used to make the dam model are quartz sand and pebbles of various sizes. The content percentage of each grain group is obtained based on the grain gradation curve shown in Fig. 3. After calculation of the total weight of the dam

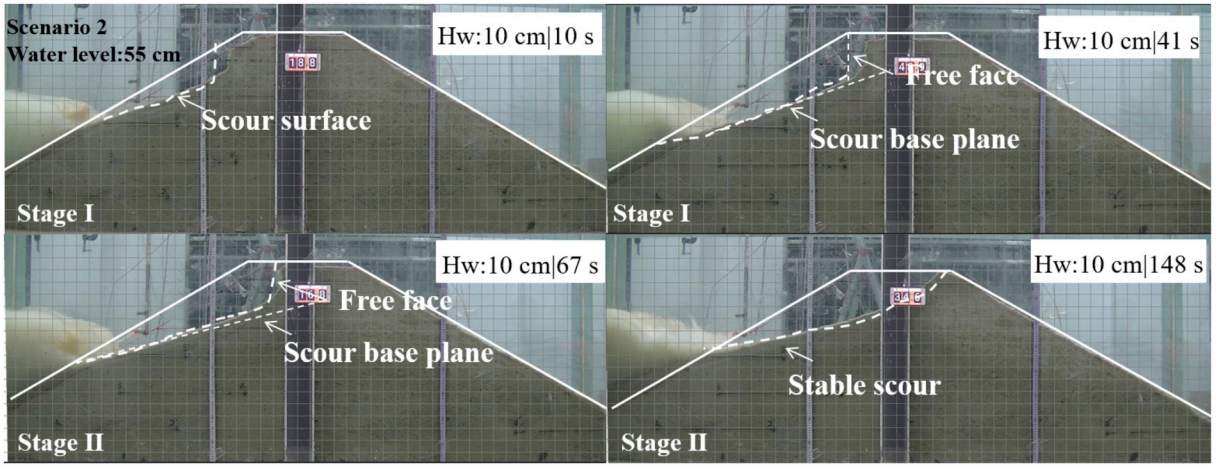

(a) Photographs of Scenario 2

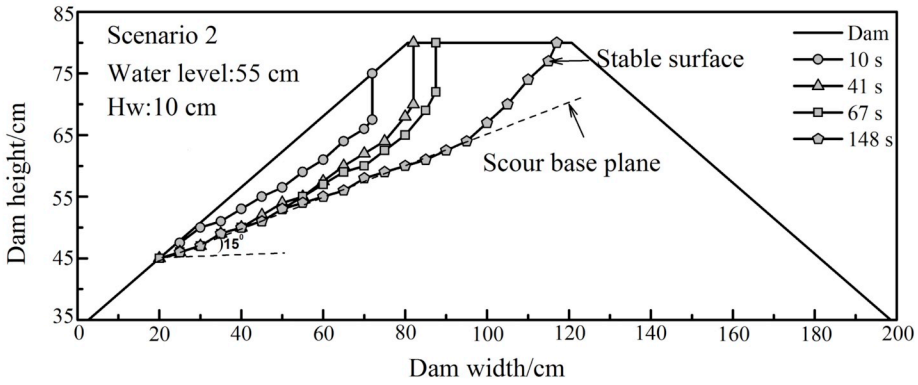

(b) Development of dam erosion in Scenario 2

Fig. 5. Scenario 2.

model, the weights of the different fractions are determined. Finally, the different fractions are fully mixed. Since a dam model needs a certain moisture content, to maintain the basic shape of the dam model, its moisture content is kept at approximately 10% by adding the appropriate amount of water into the test materials.

2.3. The experimental design

To analyze the effect of a wave on the dam stability under different water level conditions, water levels of 55 cm and 75 cm in the landslide dam lake were used in the tests, and three wave heights were set used for each water level. Limited by the maximum wave height that can be produced by the wave maker, the wave heights 5 cm, 10 cm and 20 cm are selected. When the wave period reaches 3 s, the wave shape usually displays the characteristics of an elliptic cosine wave, and the wave trough is flat, which will disturb the test results. Thus, the wave period is selected as 2 s in our tests. This leads to a sine wave shape. The parameters of the 6 test scenarios are listed in Table 1.

2.4. Test procedure

The test procedure in our study is as follows:

(1) Draw an outline on the wall of the flume according to the shape and size of the predesigned dam and overlay this with a grid. Apply the density controlled method to build the dam in consecutive layers of 10 cm thickness each. While building the dam, bury the six piezometers at the specified locations, five of which are close to the upstream slope and one is close to the downstream slope (Fig. 2).
(2) Install three cameras on the outside of the flume, one at the front of the flume and one each, upstream and downstream of the dam slope.
(3) Turn on the dynamic data acquisition instruments, adjust the piezometers to zero, and begin monitoring the data. Then fill the model lake to the target value.
(4) When the dam seepage is at a constant level, the wave spectrum is input into the wave- generating system, and the wave maker starts working. When the experimental phenomena no longer changes, stop the wave maker, the test is finished.
(5) During the entire process, the test data are being autosaved by the computer.

3. Test results

The flume model tests have shown that the landslide dam stability in the presence of surge waves is different from that under static water conditions. The stability of a dam under static conditions is determined by the water level and dam height (Peng and Zhang, 2013a, 2013b) since most of the landslide dam failures are caused by overtopping. Under surge wave conditions, the stability of a dam is determined by the difference between the effective water level and the effective dam height (ΔH).The effective water level is the sum of the water level and the overlapping wave height, which is in reality 0–2 cm higher than the wave height. The effective dam height is defined as the dam height

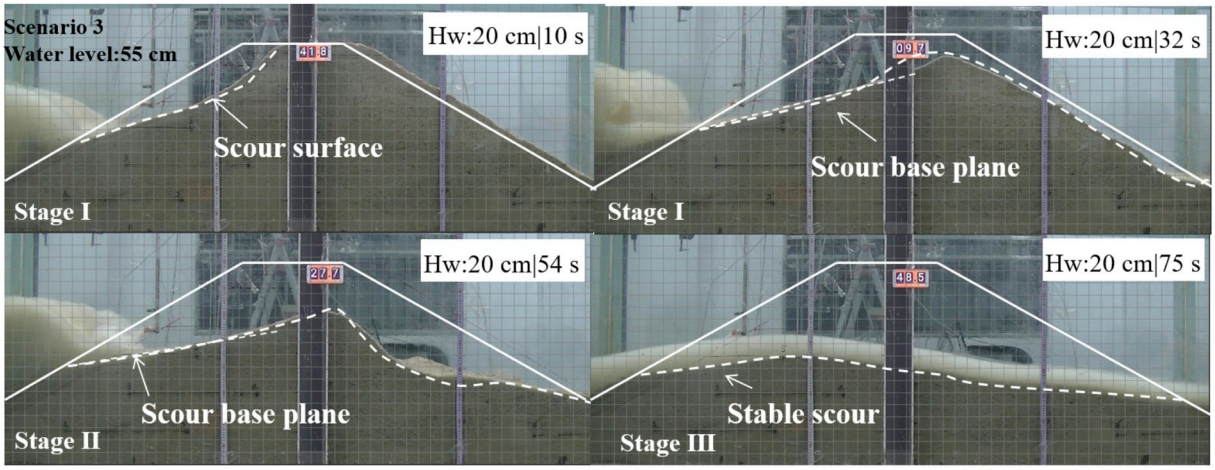

(a) Photographs of Scenario 3

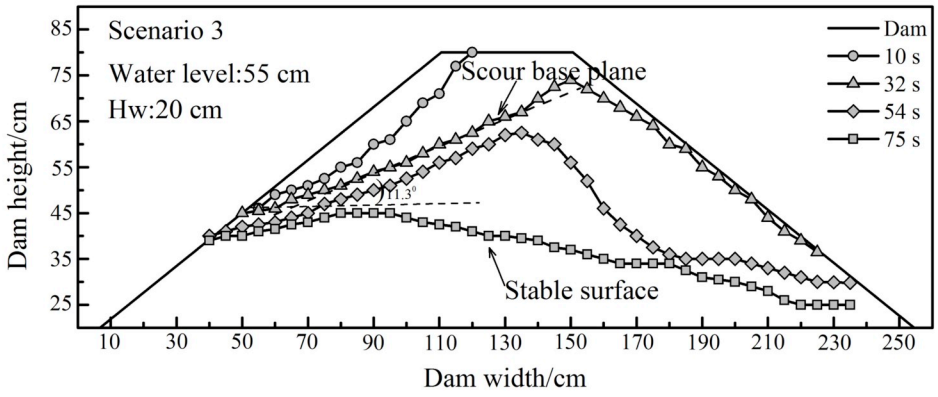

(b) Development of dam erosion in Scenario 3

Fig. 6. Scenario 3.

minus the dam height loss due to local sliding caused by the wave erosion. The dam height will not decrease until the sliding surface intersects the downstream slope. Normally, the higher the water depth or the wave height, the larger the dam height loss. As shown in Table 2, the landslide dams in Scenarios 1 and 2 remained stable as indicated by $\Delta H < 0$, while the landslide dams in Scenarios 3–6 failed as indicated by $\Delta H > 0$.

3.1. Erosion characteristics of the upstream dam slope

In all six test scenarios, the upstream dam slopes are eroded by waves. These six scenarios are divided into two modes: Scenarios 1 and 2 belong to the "stability mode", and Scenarios 3–6 belong to the "instability mode".

3.1.1. Stability mode

In Scenarios 1 and 2, the effective water level (H_{we}) is lower than the effective dam height (H_{de}), so the wave will only erode the upstream dam slope and not the downstream dam slope. The stability mode can be divided into two stages: stage I is the formation of the scour base plane, and stage II is the formation of a stable surface. In the chapters 3.1 and 3.2 the timing in sec starts with the start of the wave generation.

3.1.1.1. Scenario 1. Stage I (0–32 s) When wave-making starts, an erosion surface gradually forms uniformly over the whole width and height of the upstream dam slope, which is the scour base plane. At 32 s, the scour base plane is formed with a slope angle of 18.4°. Because the wave height is only 5 cm in this scenario, the potential for erosion is small and there is only slight erosion at the dam crest (Fig. 4a). Stage II (32–67 s) With the continuous erosion caused by the waves, an aerial surface forms on the upstream dam slope, which collapses due to gravity and a free face is formed. As the waves continue to scour the slope, the collapsing process continues and the erosion surface of the upstream slope develops further. At 67 s, the surface of the upstream dam slope becomes stable without overtopping. (Fig. 4b).

3.1.1.2. Scenario 2. Stage I (0–41 s) With a wave height of 10 cm, the waves erode the dam more intensely, and the erosion that occurs is greater than that in Scenario 1. The waves also cause an aerial surface on the upstream dam slope and eventually cause a vertical surface. The erosion surface expands as the wave action continues and a scour base plane is formed at 41 s with a slope angle of 15°. At the same time, the waves erode the crest of the dam (Fig. 5a). Stage II (41 s–148 s) As the waves erode the crest of the dam, a free face develops parallel to the scour base plane, and the width of the crest decreases. The waves can no longer cause further expansion of the erosion surface. At 148 s, the upstream dam slope forms a stable erosion surface which intersects the dam crest. (Fig. 5b).

3.1.2. Instability mode

Scenarios 3–6 are different from Scenarios 1 and 2. In scenarios 3–6, the effective water level (H_{we}) is higher than the effective dam height (H_{de}), and overtopping will occur. As a result, the wave erosion on the

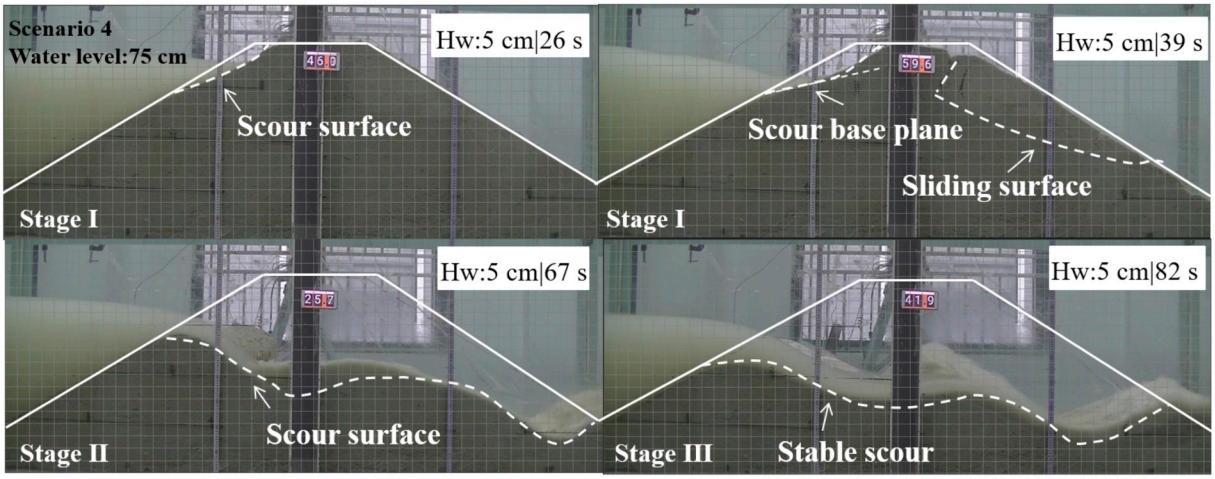

(a) Photographs of Scenario 4

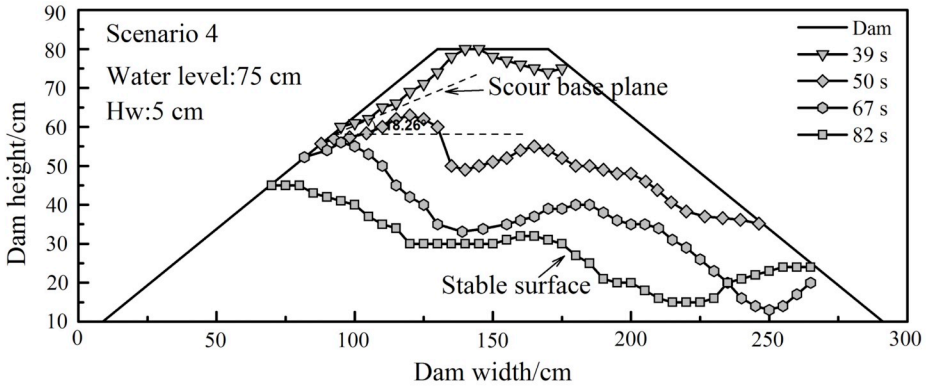

(b) Development of dam erosion in Scenario 4

Fig. 7. Scenario 4.

upstream dam slope is different from the erosion in the stability mode. The "instability" mode can be divided into three stages: stage I is the formation of the scour base plane, stage II is the disappearance of the upstream erosion surface, and stage III is the formation of a stable surface.

3.1.2.1. Scenario 3. Stage I (0–32 s) The wave height in this scenario is 20 cm. An erosion surface gradually forms on the upstream dam slope and quickly intersects with the dam crest. As the wave impact continues, the erosion surface moves downstream so that the dam crest width decreases rapidly until the crest disappears. In addition, the erosion surface also moves downward, and the angle between the erosion surface and the horizontal decreases continuously. At 32 s, the scour base plane forms a slope angle of 11.3 degrees (Fig. 6a). Meanwhile, the effective dam height (H_{de}) decreases to 73 cm, which is lower than the effective water level (H_{we} = 75 cm); and an overflow occurs. Stage II (32 s–67 s) At 54 s, the waves begin to flow turbulently downstream; as a result, the height of the dam continues to decrease, the amount of overtopping increases, and the erosion intensifies. Stage III (67 s–75 s) As the erosion surface of the upstream dam slope disappears, the downstream erosion surface intersects with the upstream dam slope. Subsequently, erosion occurs on the downstream surface, forming a relatively flat and stable erosion surface (Fig. 6b).

3.1.2.2. Scenario 4. Stage I (0–39 s) In this scenario, with a the higher water level, the erosion surface of the upstream dam slope is also higher, and the waves periodically flow over the top of the dam. The dam crest is eroded immediately, and the height of the dam body is reduced to 78 cm, such that the effective dam height (H_{de}) is lower than the effective water level (H_{we} = 80 cm). This situation leads to overtopping by the water in the reservoir lake. Meanwhile, a potential sliding surface is formed on the downstream dam slope with relatively large deformation and cracks inside the dam, which aggravates the dam height loss. At 39 s, the scour base plane is formed with a slope angle of 18.26 degrees (Fig. 7a). Stage II (39 s–67 s) As the waves continue to erode the downstream slope, the sliding surface collapses and the height of the dam decreases rapidly. Due to strong wave erosion, the upstream erosion surface disappears at 67 s. Stage III (67–82 s) As the height of the dam decreases, waves erode both upstream and downstream slopes and finally form a wave-form scouring surface (Fig. 7b).

3.1.2.3. Scenario 5. Stage I (0–20 s) In this scenario, the water level in front of the dam is 75 cm, and the wave height is increased to 10 cm. The combined water level and wave height in front of the dam is more than the height of the dam. As wave making begins, the upstream and downstream slopes are eroded simultaneously, and the width of the dam crest decreases from both sides to the center. As the wave impact continues, the scour base plane forms at 20 s with a slope angle of 15.6 degrees (Fig. 8a). Stage II (20s–75 s) The downstream dam slope is

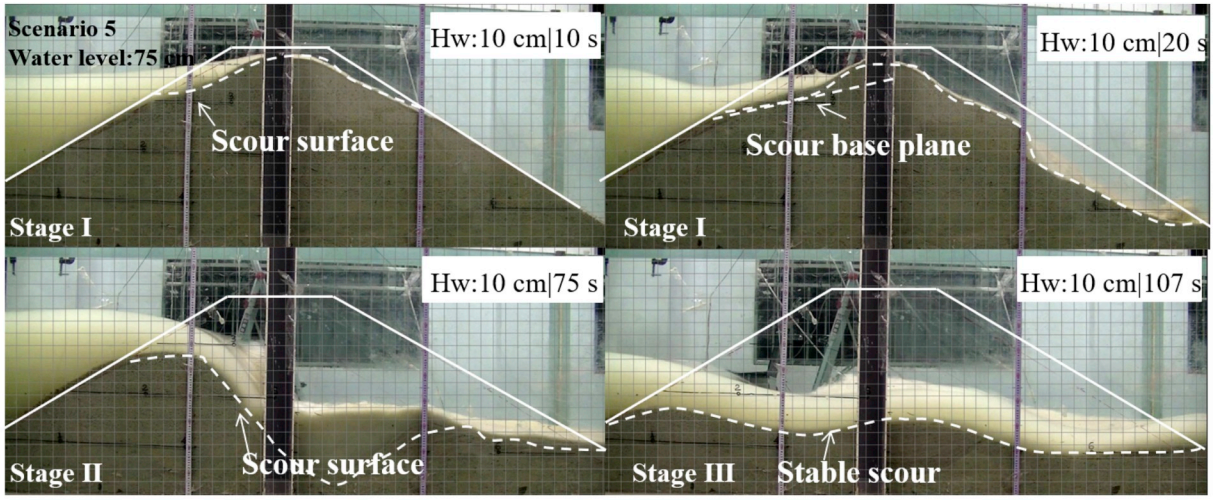

(a) Photographs of Scenario 5

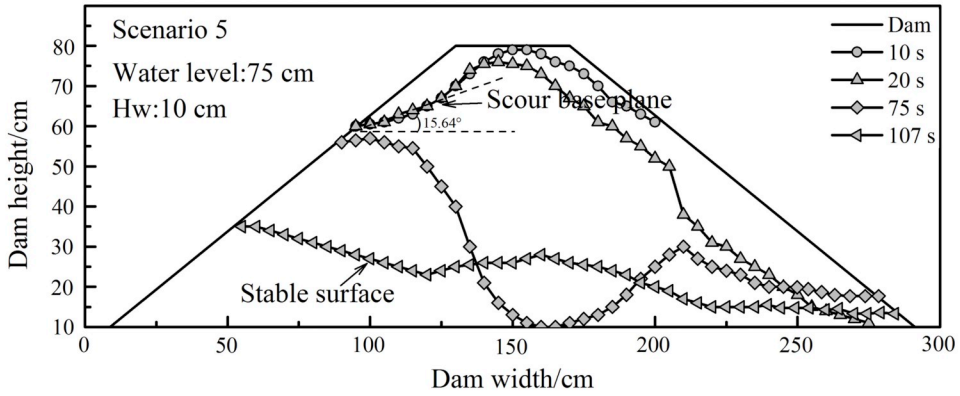

(b) Development of dam erosion in Scenario 5

Fig. 8. Scenario 5.

strongly eroded and partially collapses. Stage III (75 s–107 s) When waves wash away the upstream dam slope, the effective dam height decreases rapidly, and some materials are deposited in the eroded middle part of the dam body. Eventually, a wave-shaped stable erosion surface is formed at 107 s. The height of the residual dam body under this scenario is much less than that in Scenario 4 (Fig. 8b).

3.1.2.4. Scenario 6. The wave height is increased to 20 cm. The wave erosion process on the upstream dam slope is similar to that of Scenario 5, and can be divided into three stages. Stage I (0–28 s)

At 16 s, the cross-sectional shape of the dam changes from an echelon to roughly a triangle. The scour base plane on the upstream dam slope forms at 28 s with a slope angle of 10.2 degrees (Fig. 9a). Stage II (28 s–58 s) The middle part of the dam collapsed, but the upstream slope remains at a certain height, and the upstream erosion surface disappears at 58 s. Stage III (58 s–91 s)

Subsequently, some material is deposited in the middle part of the dam due to the continuous erosion of waves. A stable surface eventually forms on the dam body at 91 s (Fig. 9b).

3.2. Erosion characteristics of the downstream dam slope

In our study, overtopping failure did not occur in Scenarios 1 and 2, and the wave did not erode the downstream dam slope. The effective water levels (H_{we}) in Scenarios 3–6 were higher than the effective dam height (H_{de}), and the waves eroded the downstream dam slope in different ways through overtopping. The downstream dam slope erosion in these four scenarios can be divided into two modes, of which Scenarios 3–5 belong to the "nonuniform" mode and Scenario 6 belongs to the "uniform" mode.

3.2.1. Nonuniform mode

In scenarios 3–5, the waves do not erode the downstream dam slope uniformly due to relatively low values of Delta H (see Table 2). Gullies form on the downstream dam slope by local erosion. As ΔH increases during continuous erosion, higher wave energy made the gullies disappear gradually and the downstream dam slope erodes uniformly. The "nonuniform" mode can be divided into two stages: in Stage I gullies form on downstream dam slope, in Stage II the gullies disappear, and there is uniform erosion of the downstream dam slope.

3.2.1.1. Scenario 3. Stage I (0–10 s) At the beginning, the waves do not erode the downstream dam slope. However, as the waves continue, the dam decreases in height, and overtopping occurs. The waves keep eroding the central part of the downstream dam slope, and a gully forms at 10 s (Fig. 10). Stage II (10s–72s) With the continuous gully expansion and decreasing dam height, at 32 s, the amount of overtopping increases. At 46 s, the gully in the downstream dam

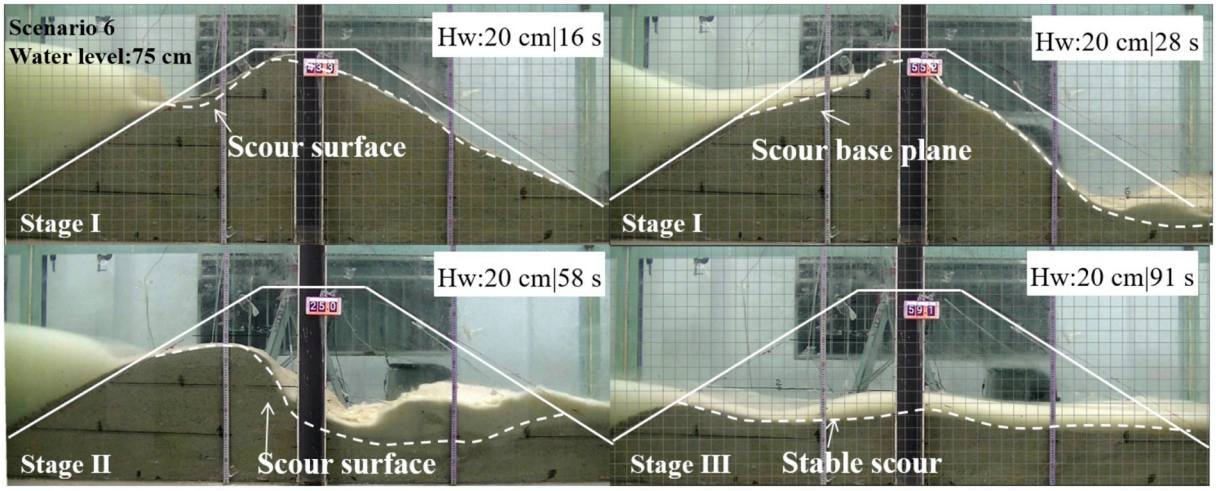

(a) Photographs of Scenario 6

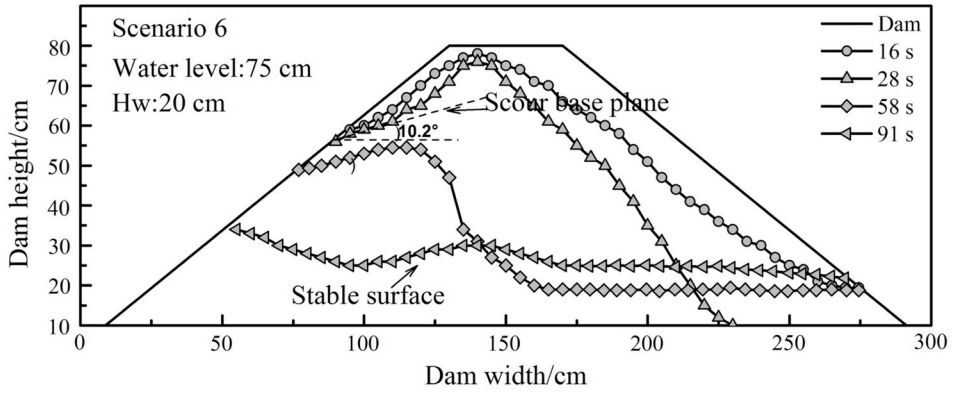

(b) Development of dam erosion in Scenario 6

Fig. 9. Scenario 6.

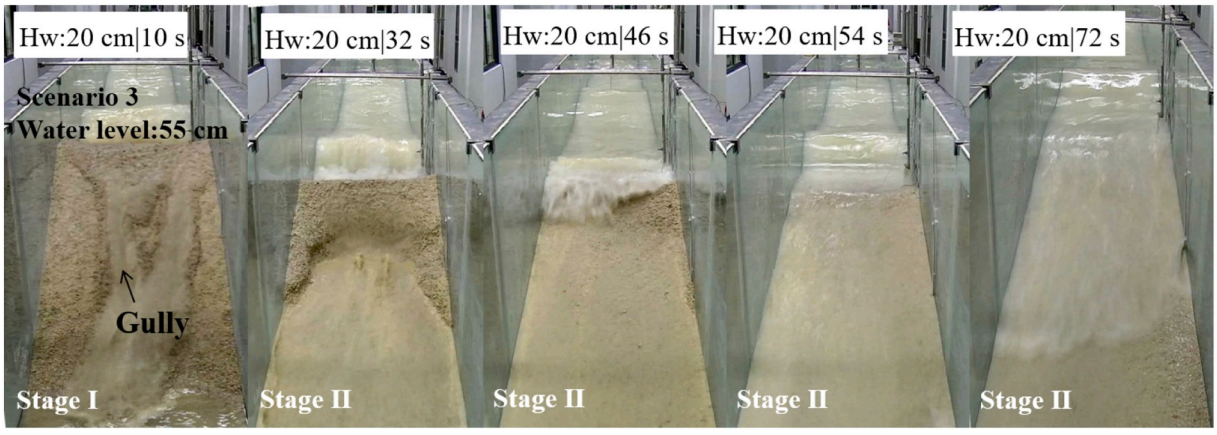

Fig. 10. Photographs of the dam breaching, from the downstream perspective, in Scenario 3.

slope disappears. After 54 s, the height of the dam body drops rapidly. The surface becomes flat, and the slope angle of the downstream dam slope decreases. At this point, the waves begin to erode the downstream dam slope uniformly.

3.2.1.2. Scenario 4. Stage I (0–19 s) As the waves continue to scour the dam, the overtopping causes two narrow gullies at 19 s (Fig. 11). At the same time, there is water seepage at the dam toe. Stage II (19 s–67 s) At 26 s, due to the water seepage, the middle part of the downstream dam slope shows a shallow sliding. The lake water overflows through the gullies, and there is also water flow on the downstream dam slope due to seepage. The downstream dam slope is further eroded in the upstream direction, and a local landslide occurs at the original position of an old sliding plane at 39 s. The downstream dam slope is seriously scoured due to the discharge increase, and the gullies are enlarged. At 47 s, the gullies disappear, and the remains of the dam and

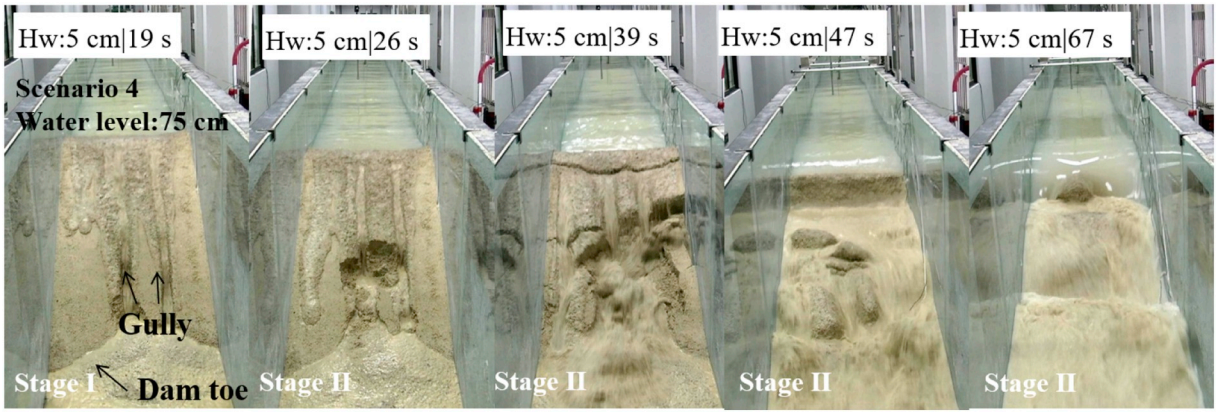

Fig. 11. Photographs of dam breaching from downstream in Scenario 4.

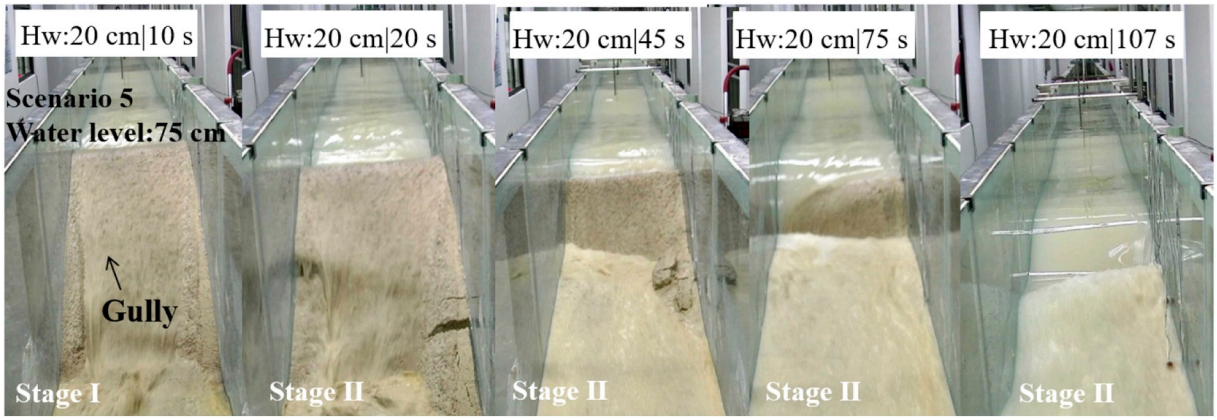

Fig. 12. Photographs of dam breaching from downstream in Scenario 5.

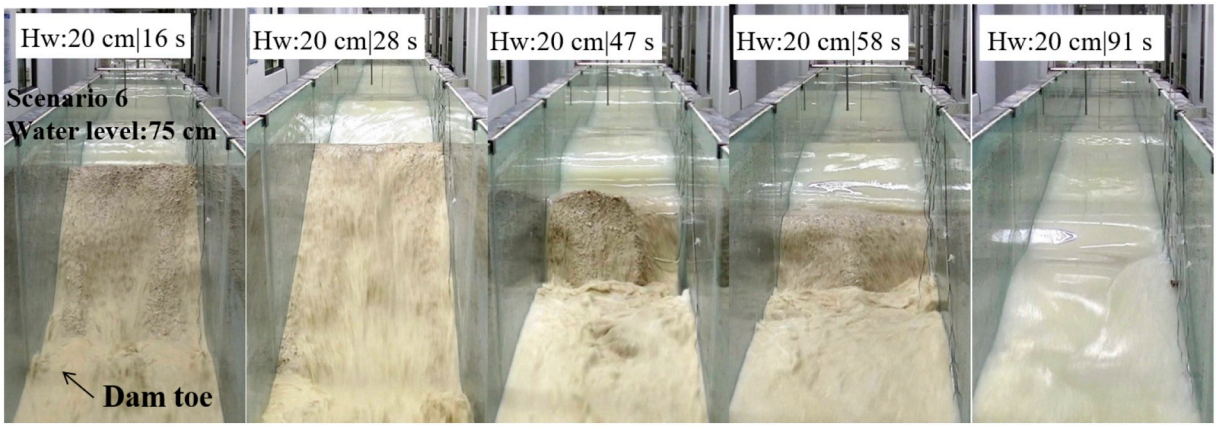

Fig. 13. Photographs of dam breaching from downstream in Scenario 6.

downstream alluvium have a wavy pattern. The subsequent waves erode the downstream dam slope uniformly.

3.2.1.3. Scenario 5. Stage I (0–10 s) The amount of wave overtopping in this scenario is larger than that in the preceding scenarios. The surge wave impact on the downstream dam slope is more intense. A wider "gully" is formed on the downstream dam slope at 10 s (Fig. 12). Stage II (10s–107 s) With the scouring and lateral expansion of the gully, the upstream reservoir water flows in large quantities, and at 20 s, the dam crest begins to settle. At 45 s, the dam failure intensifies, the height of the dam begins to decrease sharply, and the gullies disappear in the downstream dam slope. After 75 s, the peak value of the overflow has passed, the scouring action and material migration capacity decreases, and part of the dam body is deposited in situ, causing a flattened residual dam body. Then, the waves begin eroding the downstream dam slope uniformly.

3.2.2. Uniform mode

In scenario 6, the process of downstream wave erosion is different from that of Scenarios 3–5. As shown in Fig. 6, the water level is 75 cm, the wave height is 20 cm, and the height difference (ΔH) is > 21 cm, so the level of overtopping is high. The waves erode the downstream dam slope uniformly, without gullies (Fig. 13). At 16 s, the downstream scour surface has already undergone deep vertical cutting and lateral

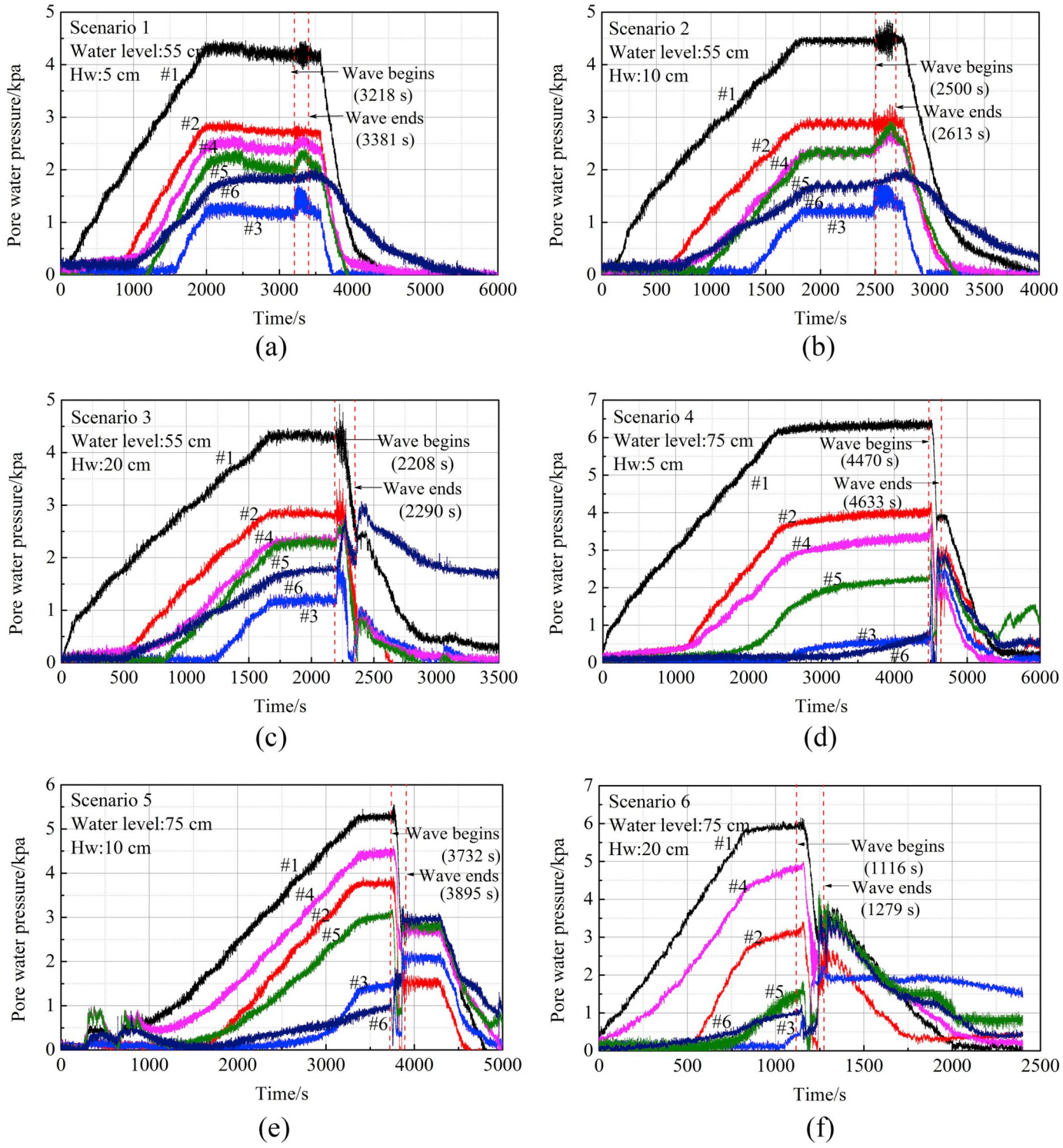

Fig. 14. Water pressures in the scenarios with different water levels and wave heights.

expansion, resulting in the settlement of the dam top. The length of the downstream dam slope decreases gradually. At 47 s, the dam breach intensifies the height of the dam begins to decrease sharply and gradually a scour surface is formed parallel to the trough bottom. Due to the scouring action, the sediment is carried away and deposited at the dam toe.

4. Pore water pressure

In our tests, six pore water pressure gauges were embedded in the dam body, of which the #1–#5 pore pressure gauges were embedded in the upstream dam slope and the #6 pore pressure gauge was embedded in the downstream dam slope (Fig. 2). The pore water pressure changes during the stages of water storage, static stage, wave generation loading and drainage (the time recording in seconds starts with the start of the reservoir filling and ends at the moment that the lake is fully drained).

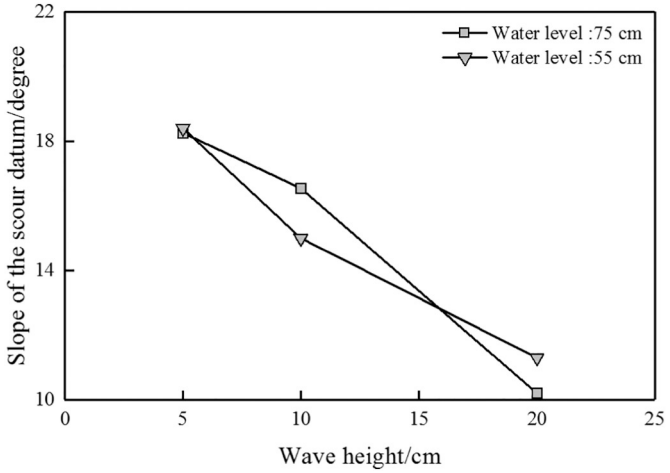

Fig. 15. Relationship between the sloping angle of the erosion scour and the wave height.

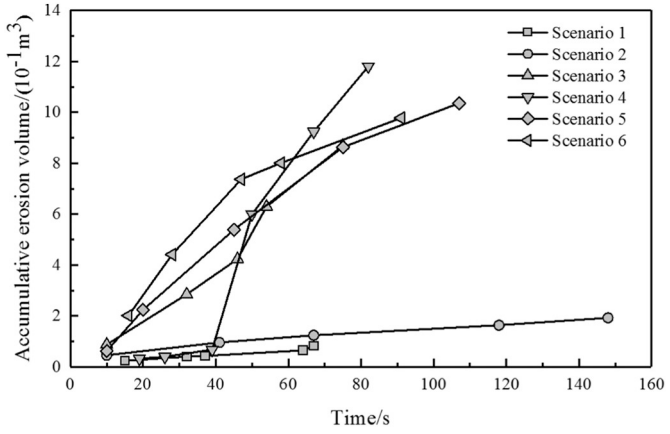

Fig. 16. Relationship between cumulative erosion volume of the dam and time.

The characteristics of the changes in the pore water pressure under various scenarios is comparatively similar. The pore water pressure has an overall downward trend during the collapse of the dam body. The effective water level in scenarios 1 and 2 is lower than the effective dam height. Only the upstream dam slope is eroded and the downstream dam slope is not eroded, so the pore pressure does not drop abruptly (Fig. 14 a b). In the other four scenarios, because of dam failure, there is a sudden drop in the pore pressure curves (Fig. 14 c, d, e and f).

In the water storage stage, the increase of the pore water pressure measured by gauges #1–#5 is similar, while that measured by #6 is lower because of the long hydraulic path. In the static stage, the pore water pressure at each measuring point is relatively stable, and related to the location of each measuring point. In the wave-making stage, the pore pressure in the dam body varies periodically per wave impact. The pore pressure near gauges #1–#3, near the upstream surface of the dam, changes greatly, which affects the strength parameters of the dam in such a way that the upstream dam slope is more easily eroded. However, the amplitude of the pore pressure variation measured at gauges #4–#6 is relatively small, and its influence on the dam stability is rather limited. During the drainage stage, the rate of decrease in the pore water pressure measured at gauges #1–#5 is the same, while that measured by gauge #6 is relatively small.

By analyzing the effect of water level and wave height on pore pressure, it is found that in the water storage and static stages, the increased amplitude of the pore water pressure at each point of the dam with a water level of 75 cm is greater than with a water level of 55 cm, indicating that the variation in the amplitude of the pore water pressure is proportional to the water level upstream of the dam. In the wave-making stage, when the water level is 55 cm, the variation in the amplitude of the pore water pressure at points #1–#3, near the upstream surface, is close to the variation in the amplitude of the wave height. However, when the water level is 75 cm, the variation in the amplitude of the pore pressure at points #1–#3 is close to 0.5 kPa, under different wave heights, due to wave overtopping. This indicates that with an increase in the water level and wave height upstream of the dam, the variation in the amplitude of the pore water pressure increases and the stability of the dam decreases.

5. Discussion

5.1. The effect of water level and wave height on erosion

Although the water level and wave height are the two components of the effective water level, the roles these parameters play are very different. The water level determines the position of the erosion on the upstream slope, while the wave height determines the erosion boundary above the water level and the energy available for erosion. Because of the erosion and local sliding caused by the waves, the inclined surface extends to the dam crest. The higher the wave is, the flatter the erosion surface will be. When the erosion surface reaches the downstream slope, the dam height is reduced, and the surge waves begin to act directly on the downstream slope. When this occurs, the dam is rapidly breaches. In Scenario 1, the erosion surface only formed on the upstream slope; in Scenario 2, the erosion surface reached the dam crest but not the downstream slope. Thus, the landslide dams in Scenarios 1 and 2 remained stable. In Scenarios 3–6, the erosion surfaces all reached the downstream slope, leading to rapid dam failure.

The breaching process of landslide dams subject to surge waves is quite different from those with a static water level. The dam breach process with a static water level, can be divided into two phases: the breach initiation phase and the breach development phase (Peng et al., 2014). The first phase starts when overflow occurs and extends to the point where there is obvious erosion on the upstream slope. The second phase starts from the end of the first phase to the end of the dam breach. Normally, the erosion in the first phase is relatively slow; while the erosion in the breach development phase is much faster, and the peak outflow rate always occurred in this phase during experiments.

The dam breaching due to surge waves is much more intense during the first phase. The dam breach longitudinal profile is S-shaped, as shown in Figs. 6–9. However, the difference in the erosion processes in the dam breach development phase is not significant because the erosion in this phase is dominated by the relatively high water level in the breach. In short, the landslide dam breach due to surge waves would proceed more quickly and requires an early warning and evacuation, while the breaching flood itself may not be noticeably enlarged.

5.2. The erosion datum angle and erosion volume

Fig. 15 shows the relationship between the slope of the erosion scour and wave height. When the water level in front of the dam is 55 cm, the angles between the erosion scour level and the water level for the wave heights of 5 cm, 10 cm and 20 cm are 18.4°, 15° and 11.3°, respectively. When the water level in front of the dam is 75 cm, the angles between the scour base plane and the horizontal plane for these three wave heights are 18.3°, 16.5° and 10.2°, respectively. The angle between the erosion datum plane and the horizontal plane decreases with increasing wave height.

Fig. 16 shows the relationship between the cumulative erosion amount of the dam and time. With increasing wave height, the cumulative erosion volume of the dam, i.e., the average erosion rate, increases with time. By comparing and analyzing the cumulative erosion volume of the dams in Scenarios 3 and 6, it is found that the average erosion rate under Scenario 6 is higher than that under Scenario 3. The

effective water level is higher and the wave overtopping amount is higher under Scenario 6, so that the erosion rate of the dam is faster. It should be noted that under Scenario 4, the erosion rate of the dam body starts increasing rapidly at 39 s, the main reason is the formation and expansion of the downstream dam slope gullies. At that time, the upper soil body of the downstream dam slope looses support and starts overall sliding.

5.3. Size and scale of the experiments

The experiments were not designed to be a scale model of a specific landslide dam. According to the research of Xu et al. (2009), Peng et al. (2014), the scale and shape of the dams formed during the Wenchuan earthquake is widely varying. The height of the dams ranges from several meters to > 100 m (such as the Laoyangyan landslide dam), and the volume of the dams ranges from tens of thousands of cubic meters to 20.4 million cubic meters (for Tangjiashan landslide dam). The purpose of this paper is to discuss the influence of the variation of the lake water level and wave height on the stability of dams in general terms, and not to study the behaviour of specific dams, so we did not use a well-defined scale factor in our experiments. The material used in our experiment is the material of Donghekou Dam, a fine-grained material. Xiao and Lin (2016) found that fine-grained dams are more easily damaged by seepage under surge (due to variations of the water pressure) than dams of other materials. As permeability has an important influence on the stability of the dam, we used in our experiments the original gradation of Donghekou Dam to ensure the consistency of permeability. In all of our experiments we used identical material. In following stages of our research program, we will conduct model tests with materials with different gradations to explore the influence of gradation on the stability of a dam.

6. Conclusion

In this paper, the effects of water level and wave height on landslide dam stability under surge wave impact are studied. The following conclusions are drawn.

(1) The landslide dam stability under the surge wave is determined by the difference (ΔH) between the effective water level (the sum of the water level and the overlapping wave height) and the effective dam height (the dam height after reduction due to local sliding). When $\Delta H < 0$, a stable eroded upstream surface was eventually formed; the erosion surface inclination angle decreased and the erosion volume increased with larger wave heights; When $\Delta H > 0$, the dam was overtopped and breached by the next waves.
(2) Although the water level and wave height are the two components of the effective water level, the roles these key factors play are clearly different. The water level determines the erosion position on the upstream slope, while the wave height determines the erosion boundary above the water level and the energy available for erosion. Due to wave erosion and local sliding, an inclined erosion surface extends to the dam crest. The higher the wave height is, the flatter the erosion surface is and the longer the erosion extends from the upstream slope. When the erosion surface reaches the downstream slope, the dam height is reduced, and the surge wave directly impacts the downstream slope.
(3) The erosion in the breach initiation phase is much faster with surge waves than at dam breach due to overtopping, while the corresponding difference in the breaching development phase is not very significant. In short, the landslide dam breach with surge waves develops more quickly, thus requiring earlier warnings and evacuation, although the breaching flood itself may not be noticeably enlarged.
(4) The pore water pressure close to the upstream slope is much more sensitive to the surge wave impact than far from the upstream slope. The variation in the amplitude of the pore pressure at measuring points, near the upstream surface, is close to the variation in the amplitude of the wave heights, but the response of the pore pressure to the surge wave impact at other points further away from the upstream dam slope is weak.

Funding

This research was supported by the National Natural Science Foundation of China (Grant Nos.41731283,41877234 and 41602287), and the Fundamental Research Funds for the Central Universities

References

Blown, I., Church, M., 1985. Catastrophic lake drainage within the Homathko River basin, British Columbia. Can. Geotech. J. 22 (4), 551–563.
Chang, D.S., Zhang, L.M., 2010. Simulation of the erosion process of landslide dams due to overtopping considering variations in soil erodibility along depth. Nat. Hazards Earth Syst. Sci. 10 (4), 933–946.
Chen, H.Y., Cui, P., Chen, X.Q., 2015. Laboratory experiments of water pressure loads acting on a downstream dam caused by ice avalanches. Landslides 12 (6), 1131–1138.
Cui, P., Zhu, Y.Y., Han, Y.S., 2009. The 12 May Wenchuan earthquake-induced landslide lakes: distribution and preliminary risk evaluation. Landslides 6 (3), 209–223.
Demirel, E., Aydin, I., 2016. Numerical simulation and formulation of wave run-up on dam face due to ground oscillations using major earthquake acceleration records. J. Eng. Mech. 142 (6), 06016001.
Evans, S.G., Clague, J.J., 1994. Recent climatic change and catastrophic geomorphic processes in mountain environments. Geomorphology 10 (3), 107–128.
Grilli, S.T., Watts, P., 1999. Modeling of waves generated by a moving submerged body. Applications to underwater landslides. Eng. Anal. Boundary Elem 23 (8), 645–656.
Hager, W.H., Fritz, H.M., Minor, H.E., 2004. Near field characteristics of landslide generated impulse waves. J. Waterw. Port Coast. Ocean Eng. 130 (6), 287–302.
Huang, W.K., Lee, C.F., Wei, L.W., 2013. DEM simulation for landslide process and barrier dam formation on the mountainous highway. Egu Gen. Assembly 15, 74–99.
Koo, W., Kim, M.H., 2008. Numerical modeling and analysis of waves induced by submerged and aerial/sub-aerial landslides. KSCE J. Civ. Eng. 12 (2), 77–83.
Lin, P., Liu, X., Zhang, J., 2015. The simulation of a landslide-induced surge wave and its overtopping of a dam using a coupled ISPH model. Eng. Appl. Comput. Fluid Mech. 9 (1), 432–444.
Liu, H.D., Xiao-Chao, L.I., Liu, S., 2013. Zhouqu catastrophic mudslide barrier dam stability. Analysis Yellow River 142 (12), 04016059.
Madsen, O.S., 1978. Wave-induced pore pressures and effective stresses in a porous bed. Géotechnique 28 (4), 377–393.
Niu, Z.P., Xu, W.L., Li, N.W., 2012. Experimental investigation of the failure of cascade landslide dams. Hydrodyn. Stud. Adv. 24 (3), 430–441.
Peng, M., Zhang, L.M., 2012. Breaching parameters of landslide dams. Landslides 9 (1), 13–31.
Peng, M., Zhang, L.M., 2013a. Dynamic decision making for dam-break emergency management - part 1: theoretical framework. Nat. Hazards Earth Syst. Sci. 13 (2), 425–437.
Peng, M., Zhang, L.M., 2013b. Dynamic decision making for dam-break emergency management - part 2: application to Tangjiashan Landslide Dam failure. Nat. Hazards Earth Syst. Sci. 13 (2), 439–454.
Peng, M., Zhang, L.M., Chang, D.S., Shi, Z.M., 2014. Engineering risk mitigation measures for the landslide dams induced by the 2008 Wenchuan earthquake. Eng. Geol. 180 (4–5), 68–84.
Risley, J.C., Walder, J.S., Denlinger, R.P., 2006. Usoi dam wave overtopping and flood routing in the Bartang and Panj Rivers, Tajikistan. Nat. Hazards 38 (3), 375–390.
Sattar, A., Konagai, K., Kiyota, T., 2012. Measurement of debris mass changes and assessment of the dam-break flood potential of earthquake-triggered Hattian landslide dam. Landslides 8 (2), 171–182.
Shi, Z.M., Wang, Y.Q., Peng, M., Chen, J.F., Yuan, J., 2014. Characteristics of the landslide dams induced by the 2008 Wenchuan earthquake and dynamic behavior analysis using large-scale shaking table experiments. Eng. Geol. 194, 25–37.
Shi, Z.M., Wang, Y.Q., Peng, M., Guan, S.G., Chen, J.F., 2015. Landslide dam deformation analysis under aftershocks using large-scale shaking table tests measured by video grammetric technique. Eng. Geol. 186 (2015), 68–78.
Soares-Frazão, S., Zech, Y., 2007. Experimental study of dam-break flow against an isolated obstacle. J. Hydraul. Res. 45 (s), 27–36.
Tang, C.J., Lee, J.F., 1992. Landslide-Generated Waves in Reservoirs. Engineering Mechanics. ASCE, pp. 220–223.
Waragai, T., Kajiyama, T., 2011. Expansion of a landslide-dammed lake following a catastrophic landslide in January 2010 at Atabad, northern Pakistan. J. Geogr. 120 (6), 993–1002.
Wiegel, R.L., 1970. Water waves generated by landslides in reservoirs. Proc. ASCE 96 (2), 307–333.
Xiao, H., Lin, P., 2016. Numerical modeling and experimentation of the dam-overtopping process of landslide-generated waves in an idealized mountainous reservoir. J. Hydraul. Eng. 142 (12), 04016059.

Xiong, X., Shi, Z.M., Guan, S.G., 2018. Failure mechanism of unsaturated landslide dam under seepage loading – model tests and corresponding numerical simulations[J]. Soils Found. 58 (5), 1133–1152.
Xu, Q., Fan, X.M., Huang, R.Q., 2009. Landslide dams triggered by the Wenchuan Earthquake, Sichuan Province, south west China. Bull. Eng. Geol. Environ. 68 (3), 373–386.
Xu, F.G., Yang, X.G., Zhou, J.W., 2015. Experimental study of the impact factors of natural dam failure introduced by a landslide surge. Environ. Earth Sci. 74 (5), 4075–4087.
Yamamoto, T., Koning, H.L., Sellmeler, H., Van, H.E., 1978. On the response of a poro-elastic bed to water waves. J. Fluid Mech. 87, 193–206.
Yang, F.G., Zhou, X.Q., Liu, X.N., 2011. Experimental study of breach growth processes in sand dams of Quake lakes. J. Earthq. Tsunami 5 (5), 445–459.
Zhou, G.G.D., Cui, P., Chen, H.Y., 2013. Experimental study on cascading landslide dam failures by upstream flows. Landslides 10 (5), 633–643.
Zhou, G.G.D., Cui, P., Zhu, X., 2015. A preliminary study of the failure mechanisms of cascading landslide dams. Int. Sediment Study 30 (3), 223–234.